Improving the alkalophilic performances of the Xyl1 xylanase from Streptomyces sp. S38: Structural comparison and mutational analysis

Frédéric De Lemos Esteves, Thierry Gouders, Josette Lamotte-Brasseur, Sébastien Rigali and Jean-Marie Frère

Protein Sci. 2005 14: 292-302
Access the most recent version at doi:10.1110/ps.04978705

Improving the alkalophilic performances of the Xyl1 xylanase from *Streptomyces* sp. S38: Structural comparison and mutational analysis

FRÉDÉRIC DE LEMOS ESTEVES, THIERRY GOUDERS, JOSETTE LAMOTTE-BRASSEUR, SÉBASTIEN RIGALI, AND JEAN-MARIE FRÈRE

Centre d'Ingénierie des Protéines, Institut de Chimie, B6a, Université de Liège, Sart Tilman, B-4000 Liège, Belgium.

(RECEIVED July 8, 2004; FINAL REVISION September 23, 2004; ACCEPTED September 30, 2004)

Abstract

Endo-β-1,4-xylanases of the family 11 glycosyl-hydrolases are catalytically active over a wide range of pH. Xyl1 from *Streptomyces* sp. S38 belongs to this family, and its optimum pH for enzymatic activity is 6. Xyn11 from *Bacillus agaradhaerens* and XylJ from *Bacillus* sp. 41M-1 share 85% sequence identity and have been described as highly alkalophilic enzymes. In an attempt to better understand the alkalophilic adaptation of xylanases, the three-dimensional structures of Xyn11 and Xyl1 were compared. This comparison highlighted an increased number of salt-bridges and the presence of more charged residues in the catalytic cleft as well as an eight-residue-longer loop in the alkalophilic xylanase Xyn11. Some of these charges were introduced in the structure of Xyl1 by site-directed mutagenesis with substitutions Y16D, S18E, G50R, N92D, A135Q, E139K, and Y186E. Furthermore, the eight additional loop residues of Xyn11 were introduced in the homologous loop of Xyl1. In addition, the coding sequence of the XylJ catalytic domain was synthesized by recursive PCR, expressed in a *Streptomyces* host, purified, and characterized together with the Xyl1 mutants. The Y186E substitution inactivated Xyl1, but the activity was restored when this mutation was combined with the G50R or S18E substitutions. Interestingly, the E139K mutation raised the optimum pH of Xyl1 from 6 to 7.5 but had no effect when combined with the N92D substitution. Modeling studies identified the possible formation of an interaction between the introduced lysine and the substrate, which could be eliminated by the formation of a putative salt-bridge in the N92D/E139K mutant.

Keywords: endo-β-1,4-xylanase; alkalophilicity; site-directed mutagenesis; recursive PCR; docking; structural analysis

Xylan is the main component of hemicellulose and is composed of β-1,4-linked xylopyranose chains with 4-O-methyl-D-glucuronic acid, arabinose, O-acetyl, and uronic acids subtituents (Singh et al. 2003). Its complete hydrolysis requires a whole battery of enzymes among which endo-β-1,4-xylanases are preponderant. On the basis of sequence similarities and hydrophobic cluster analysis, endo-β-1,4-xylanases have been mainly grouped in families 10 and 11 of the glycoside hydrolases, although other families including families 5, 7, 8, and 43 also contain some xylanolytic enzymes (Henrissat and Davies 1997; Wong et al. 1988; Collins et al. 2004). Family 10 xylanases exhibit eightfold α/β barrel structures and have molecular masses >30,000, whereas family 11 xylanases have an all β-strand sandwich fold structure resembling a partly closed "right hand" and a lower molecular mass of ~20,000 (Torronen et al. 1994; Dominguez et al. 1995). Endo-β-1,4-xylanases (EC 3.2.1.8) are widely used in baking and industrial processes such as the clarification of fruit juices, waste treatment, and the bio-bleaching of paper pulp (Kulkarni et al. 1999). In this

Reprint requests to: Jean-Marie Frère, Centre d'Ingénierie des Protéines, Institut de Chimie, B6a, Université de Liège, Sart Tilman, B-4000 Liège, Belgium; e-mail: jmfrere@ulg.ac.be; fax: 32-4-366-33-64.

Article and publication are at http://www.proteinscience.org/cgi/doi/10.1110/ps.04978705.

latter application, the removal of lignin is facilitated by xylan hydrolysis, thereby reducing the utilization of environmentally toxic chlorinated chemicals (Viikari et al. 1994). However, pulp bleaching is performed at high temperature and high pH. Hence, xylanases to be used in this process should exhibit high stability and high activity in these extreme conditions (Kulkarni et al. 1999; Subramaniyan and Prema 2000). Although family 11 enzymes show very closely related three-dimensional structures, they can be separated into acidic and alkaline pI enzymes. Optimum pH values are highly variable within this family and range between pH 2.0 and 6.0 for acidophilic xylanases and between pH 4.0 and pH 11.0 for the so-called alkaline xylanases (Joshi et al. 2000). In both cases, the catalytic mechanism involves two glutamic acids located on either side of the cleft, which function as the nucleophile and acid/base catalyst (Miao et al. 1994; Wakarchuk et al. 1994). Site-directed mutagenesis studies on acidophilic adaptation have highlighted the importance of residues located in the neighborhood of these glutamic acids, in particular in the thumb and at the edge of the cleft (Fushinobu et al. 1998; Joshi et al. 2000; de Lemos Esteves et al. 2004). Interestingly, some alkaline xylanases show broader pH activity profiles with optima located near neutral pH (Irwin et al. 1994; Morris et al. 1998; Liu et al. 2002). Recent mutagenic studies of some of these xylanases have demonstrated the involvement of several important residues in their broader alkalophilic activity profile (Chen et al. 2001; Liu et al. 2002). Moreover, site-directed mutagenesis experiments on the *Trichoderma reesei* xylanase Xyn11 showed that the combined introduction of five arginine residues at the "Ser/Thr" surface of "the fingers" slightly elevated the optimum pH of the enzyme (0.5–1.0 pH units) (Turunen et al. 2002). Only the endo-β-1,4-xylanases Xyn11 from *Bacillus agaradhaerens* and XylJ from *Bacillus* sp. 41M-1 have been described as highly alkalophilic in family 11 xylanases (Nakamura et al. 1993; Sabini et al. 1999; Joshi et al. 2000).

Xyl1 from *Streptomyces* sp. S38 is optimally active around pH 6.0 and has potential applications in bleaching and delignification processes (Georis et al. 2000b). Recently, we investigated the molecular adaptation of endo-β-1,4-xylanases to acidophilic conditions by structural comparison of Xyl1 and the *Aspergillus kawachii* xylanase XynC (de Lemos Esteves et al. 2004). In the present work, we compare the three-dimensional structures of Xyl1 and Xyn11. On the basis of this comparison and to better understand the mechanistic adaptation of endo-β-1,4-xylanases to high alkaline conditions, site-directed mutagenesis was performed on Xyl1. In addition, the coding sequence of the XylJ catalytic domain was synthesized by recursive PCR and produced in a *Streptomyces* host. The activity profiles of the Xyl1 wild-type and mutant proteins as well as of XylJ were compared.

Results

Comparison of Xyl1 with alkalophilic endo-β-1,4-xylanases

The amino acid sequences of the catalytic domains of nine family 11 alkaline endo-β-1,4-xylanases have been aligned with Xyl1 (Fig. 1). Xyn11 from *B. agaradhaerens* and XylJ from *Bacillus* sp. 41M-1 have very similar catalytic domain sequences displaying 85% identity and are described as highly alkalophilic enzymes. The eight other xylanases are optimally active in the neutral pH range, and many differences are noted between these enzymes and the alkalophilic xylanases. In addition, superposition of the three-dimensional structures of Xyl1 and Xyn11 demonstrated a number of important structural differences but also a remarkable conservation of aromatic amino acids inside and at the edge of the catalytic cavity. Indeed, despite the fact that both Tyr185 and Tyr194 are in different orientations in the considered xylanases, residues Trp20, Tyr87, Trp89, Tyr98, Tyr128, Trp149, Tyr185, and Tyr194 are strictly conserved. However, the catalytic site of Xyn11 contains more charged residues, with Asp16, Glu18, and Glu186 corresponding to Tyr16, Ser18, and Tyr186 in Xyl1, and it has already been suggested that these residues influence the optimum pH of XylJ (Fig. 2A,B; Tamanoi et al. 1998). Moreover, Arg50 in Xyn11 is replaced by a glycine residue in Xyl1, and Asp92, which is only found in the alkalophilic xylanases, is replaced by Asn. Interestingly, some of these charged residues are present in the amino acid sequences of *Bacillus pumilus* A-30 XYNA and, to a lesser extent, in *Dictyoglomus thermophilum* Rt46B.1 XynB. This latter is optimally active at pH 6.5 and presents >50% activity between pH 5.0 and 8.0, whereas XYNA displays optimal activity near pH 6.7 and presents a broader pH activity profile with >50% activity between pH 5.5 and 9.5 (Morris et al. 1998; Liu et al. 2002). Superposition of the structures of Xyl1, Xyn11, and XynB did not indicate any major differences in the configuration of the thumb. However, XYNA and both alkalophilic xylanases present an eight-residue-longer loop between β-strands B3 and A5, whereas this loop is three residues shorter in XynB (Figs. 1, 2). In this longer loop, Lys54 protrudes into the catalytic cavity, whereas Glu57, found in Xyn11 and XylJ, points toward the thumb and is connected by a salt-bridge to the lysine residue in position 139 (Fig. 2D). Inspection of the catalytic site of Xyn11 showed that Glu18, Arg50, Lys54, and Glu186 are connected by four salt-bridges and are located in the substrate binding area. Xyn11 contains 10 salt-bridges, whereas only two and five of these are found in Xyl1 and XynB, respectively (Table 1). Furthermore, XYNA possesses eight and XylJ seven putative salt-bridges similar to those found in Xyn11. Interestingly, salt-bridge 4 is only found in Xyn11 and probably also in XylJ, while the E139–K142 interaction is specific to Xyl1.

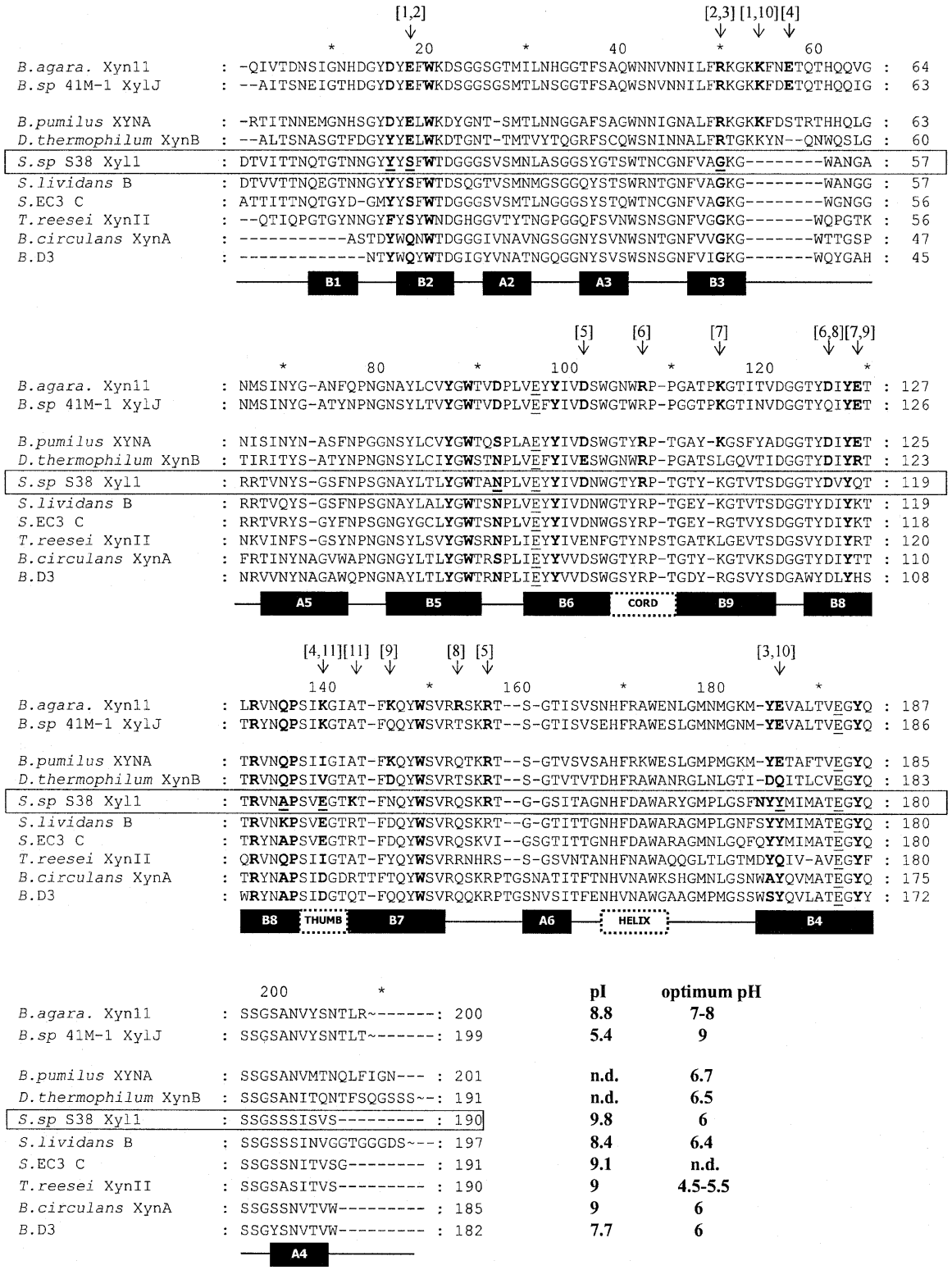

Figure 1. Sequence alignment of family 11 xylanases. The two alkalophilic enzymes are from *B. agaradhaerens* (Xyn11) (Sabini et al. 1999) and *Bacillus* sp. 41M-1 (XylJ) (Nakamura et al. 1993). The "neutrophilic" enzymes are from *B. pumilus* (XYNA) (Liu et al. 2002), *D. thermophilum* (XynB) (Morris et al. 1998), *Streptomyces* sp. S38 (Xyl1) (Georis et al. 2000a), *Streptomyces lividans* (XlnB) (Kluepfel et al. 1990), *Streptomyces* EC3 (XlnC) (Mazy-Servais et al. 1996), *Trichoderma reesei* (XynII) (Torronen et al. 1992), *Bacillus circulans* (XynA) (Yang et al. 1989), and *Bacillus* D3 (Harris et al. 1997). The residues referred to in the text are in bold, the catalytic Glu residues are underlined, and the mutated residues are in bold and underlined. The individual numbering of each enzyme is shown. In the text, the standard numbering resulting from the alignment is used consistently. Numbering indicated in brackets refers to the salt-bridges numbering (see Table 1). N.d. indicates not determined.

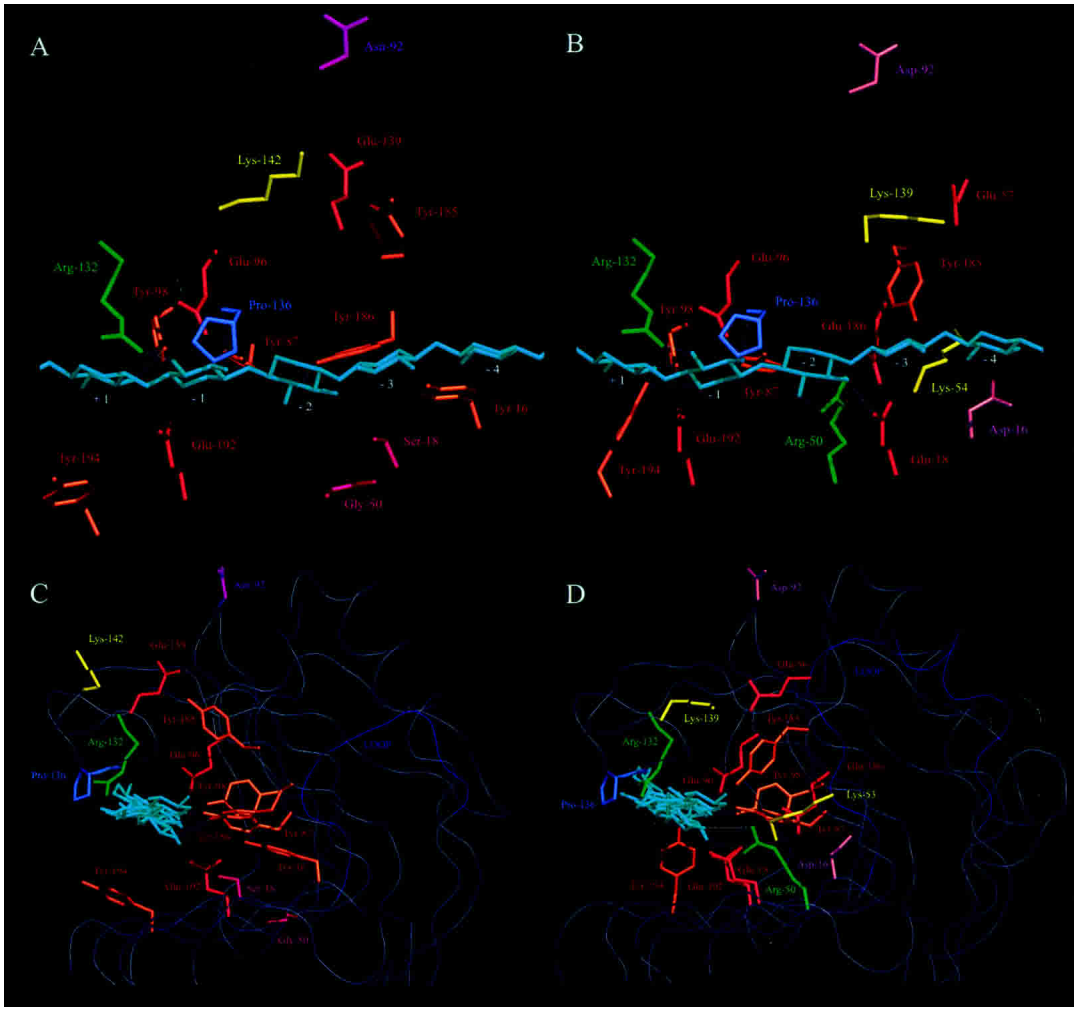

Figure 2. Docking of a chain of eight xylose residues in the active site of Xyl1 and Xyn11. Five of the eight xylose residues were accommodated in the catalytic sites of Xyl1 (*A*, *C*) and Xyn11 (*B*, *D*). (*C*, *D*) Ninety-degree presentations of *A* and *B*, respectively. The geometry of the complex was optimized by energy minimization.

Site-directed mutagenesis of the xyl1 *gene*

Based on the comparison of Xyl1 with both alkalophilic xylanases, eight residues located in the catalytic cleft were chosen for mutation. Substitutions Y16D, S18E, V48L, G50R, N92D, A135Q, E139K, and Y186E were introduced in the wild-type enzyme Xyl1, and combined mutations were investigated with mutants Y16D/S18E, S18E/Y186E, G50R/Y186E, N92D/E139K, Y16D/S18E/Y186E, and S18E/G50R/Y186E. Moreover, replacement of the loop between β-strand B3 and A5 by the homologous eight-residue-longer sequence found in XylJ and Xyn11 was performed, and in order to create the salt-bridge present in the alkalophilic enzyme, a combination of the introduced loop with the point mutation E139K was also constructed.

Preliminary characterization of the synthetic XylJ and Xyl1 recombinants proteins

The XylJ xylanase and the recombinant proteins were expressed in *Streptomyces parvulus* as previously described by Georis et al. (2000a) and ~5 mg of each protein were obtained. Mutants bearing the Y16D mutation were produced but unstable: Xylanolytic activity was detected in culture supernatants but rapidly decreased. Furthermore, the recombinant Y186E protein and mutants bearing the longer loop were secreted but inactive. The active recombinant proteins were purified and assayed for optimum temperature activity at 40°C, 50°C, 60°C, and 70°C. No modification of the optimum temperature activity was observed when compared with the wild-type, and activity measurements were performed at 50°C.

Table 1. *Comparison of the side-chain interactions in some family 11 xylanases*

Salt-bridge	Xyn11	XYNA	XylJ	Xyl1	XynB	Std. numbering
[1]	**Glu17-Lys53**	**(Glu17-Lys52)**	**(Glu16-Lys52)**	*Ser18/—*	*Glu16/Lys51*	18–54
[2]	**Glu17-Arg49**	**(Glu17-Arg48)**	**(Glu16-Arg48)**	*Ser18/Gly50*	**Glu16-Arg47**	18–50
[3]	**Arg49-Glu178**	**(Arg48-Glu176)**	**(Arg48-Glu177)**	*Gly50/Tyr171*	*Arg47/Gln174*	50–186
[4]	**Glu56-Lys136**	*Ser55/Ile134*	**(Glu55-Lys135)**	*—/Glu128*	*—/Val132*	57–139
[5]	**Asp99-Arg152**	**(Asp98-Arg150)**	**(Asp98-Arg151)**	**Asp92-Arg144**	**Glu95-Arg148**	101–156
[6]	**Arg105-Asp123**	**(Arg104-Asp121)**	*Arg104/Gln122*	**Arg98-Asp115**	**Arg101-Asp119**	107–126
[7]	**Lys112-Glu126**	**(Lys110-Glu124)**	**(Lys111-Glu125)**	*Lys104/Gln118*	*Leu108/Arg122*	115–129
[8]	**Asp123-Arg149**	*Ile122/Gln147*	*Gln122/Thr148*	*Asp115/Gln141*	*Asp119/Asp138*	126–153
[9]	**Glu126-Lys142**	**(Glu142-Lys140)**	*Glu125/Gln141*	*Gln118/Asn134*	**Arg122-Asp138**	129–146
[10]	**Lys53-Glu178**	**(Lys52-Glu176)**	**(Lys52-Glu177)**	*—/Tyr171*	**Lys51-Asp173**	54–186
[11]	*Lys136/Ala139*	*Ile134/Ala137*	*Lys135/Ala138*	**Glu128-Lys131**	*Val132/Ala135*	139–142

Xyn11 indicates *Bacillus agaradhaerens;* XYNA, *Bacillus pumilus;* XylJ, *Bacillus* sp. 41M-1; Xyl1, *Streptomyces* sp. S38; and XynB, *Dictyoglomus thermophilum.*

Salt-bridges in the wild-type enzymes are in bold. The corresponding residues that cannot form salt-bridges are shown in italics. The corresponding residues that can form putative salt-bridges are indicated in brackets. The individual numbering of each enzyme is used, but the last column shows the standard numbering of Figure 1.

pH profiles of the purified proteins

Activity of the purified proteins was determined between pH 2 and 11. With the exception of the E139K mutant and the synthetic XylJ, the purified recombinant proteins displayed activity profiles nearly identical to that of the wild-type Xyl1 enzyme. XylJ and the mutant E139K had a broader pH profile with optima near pH 7 and 7.5, respectively (Fig. 3). In addition, at the optimum pH of the wild-type enzyme (pH 6.0), XylJ and E139K presented 85% and 75% of their maximum activity, respectively. Interestingly, at pH 9, where the wild-type enzyme is almost inactive, XylJ and E139K retained 40% and 80%, respectively, of their maximum activities. The N92D substitution abolished the alkalophilic effect conferred by the E139K mutation, and more importantly, when the S18E and/or G50R substitutions was combined with the Y186E mutation, the activity of the inactive recombinant Y186E protein was restored (Table 2). In comparison to the wild-type enzyme Xyl1 (2100 ± 200 IU/mg), the E139K mutant displayed slightly lower specific activity, with 1800 ± 150 IU/mg, whereas XylJ was ~10-fold less active, with 225 IU/mg at optimum pH. At pH 10, the specific activity of the E139K protein was ~1500 IU/mg versus <100 IU/mg for the wild-type enzyme.

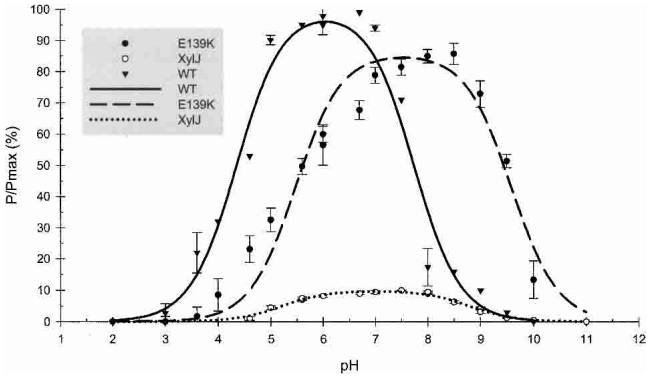

Figure 3. pH dependence of the activity of the wild-type Xyl1, the mutant enzyme E139K. and the synthesized xylanase XylJ. The solid lines were obtained by fitting the experimental data to equation:

$$P/P_{max} = \frac{100}{\frac{H^+}{K_1} + 1 + \frac{K_2}{H^+}}$$

P represents the activity of the three xylanases measured at various pH, and P_{max} the maximum activity observed for the wild-type Xyl1 at pH 6.0, corresponding to a specific activity of 2100 IU/mg of protein. pKa values of 4 and 7 were used to fit the equation.

Xyl1 and Xyn11 enzyme-substrate interactions

A chain of eight xylose residues was docked into the active sites of Xyl1 and Xyn11 on the basis of the crystal structure of *B. agaradhaerens* Xyn11, and the geometry of the complex was optimized by energy minimization (Fig. 2A,B). As mentioned above, the catalytic cavity of Xyn11 contains more charged residues involved in substrate binding. However, some interactions at subsites −1 and +1 are strictly conserved. For instance, Arg132 is hydrogen bonded to the xylose ring at subsites +1 and −1, while Tyr98 and the carbonyl group of Pro136 also interact with the xylose unit in subsites +1 and −1, respectively. Interestingly, Tyr186 in Xyl1 seems to bind the xylose ring at subsite −2, whereas the corresponding residue in Xyn11 (Glu186) is too far from the substrate to make any interaction. Moreover, binding of the substrate seems to involve more residues in Xyn11. Actually, Arg50, Tyr87, and Glu18 interact with hydroxyl groups of the xylose ring at subsite −2. In addition, Tyr194, which was found to adopt two different orientations in the native structure, is hydrogen bonded to xylose rings at both subsites −1 and +1.

Table 2. *Optimum pH and specific activities of the wild-type Xyl1 and modified enzymes*

	Optimum pH	Specific activity at optimum pH (Ul/mg)	Specific activity (Ul/mg)		pKas used in the fit
			pH 5	pH 9	
Xyl1 WT	6	2100 ± 200	1500	100	4.3/7.7
N92D	6	1850 ± 120	1500	460	4.2/8
E139K	7.5	1800 ± 150	450	1500	5.7/9.4
Y186E	—	—	—	—	—
S18E/Y186E	6	2000 ± 150	1740	<40	4.6/7.3
G50R/Y186E	5.8	1890 ± 140	1730	<40	4.6/7
N92D/E139K	5.9	1780 ± 200	1370	<40	4.6/7.1
S18E/G50R/Y186E	6	1880 ± 160	960	<40	4.9/6.7
XylJ	7	225 ± 30	85	90	5.2/8.8

Modeling of the E139K mutant

The E139K substitution eliminated the salt-bridge between Glu139 and Lys142, and it could be expected that the orientations of both side-chains would be changed by charge repulsion. However, it seems that the contribution of the E139K mutation to the alkalophilicity of the mutant did not result in any deformation of the C-α backbone of the thumb. The E139K substitution can lead to several orientations of the Lys139 and Lys142 side-chains, but most of these tend to point to the solvent, outside the cleft. Modeling showed that the side-chain of Lys142, situated in the neighborhood of the nucleophile (14.45 Å), could not be reoriented into the catalytic cavity to form interactions with Glu96 or directly influence its pK_a. Nevertheless, the introduced Lys139 is located at the edge of the thumb, and due to the flexibility of the enzyme, creation of an interaction between this residue and the substrate would be likely. Moreover, this putative interaction may be removed when the N92D mutation is combined with E139K, which allows the formation of a putative salt-bridge (3.3 Å). Furthermore, modeling also showed that a hydrogen bond could be established between the introduced Lys139 and Asn184. However, creation of this interaction requires a 120° rotation of the side-chain of Tyr185 around the Cα–Cβ bond accompanied by a motion of Tyr 186, leading to an increased distance between the latter residue and the substrate. In this situation, Tyr185 could point into the catalytic cavity and residue 186 would be unable to interact with the xylose ring in subsite −2, as observed for both homologous residues in Xyn11. Formation of the Lys139–Asn184 hydrogen bond would thus result in a situation that closely mimics that which prevails in the alkalophilic protein.

Discussion

Endo-β-1,4-xylanases (EC 3.2.1.8) are used in many industrial applications where extremes temperature and pH are often crucial and unavoidable (Harris et al. 1997). Among these processes, utilization of xylanases in the bio-bleaching of paper pulp allows reduced production of lasting and toxic organochlorine compounds in effluents (Viikari et al. 1994). However, pulp bleaching requires low-molecular-mass xylanases, which are active and stable in the akalophilic pH range, yet few natural family 11 alkalophilic xylanases are known. In fact, XylJ and Xyn11 from *Bacillus* sp. 41M-1 and *B. agaradhaerens*, respectively, are almost the only alkalophilic members of family 11, and the percentage identity between the two catalytic domains (85%) is high enough to consider these xylanases as nearly identical. Xyl1 belongs to the same family but is a "neutrophilic" xylanase with an optimum pH of ~6. An amino acid sequence alignment indicated a longer loop between β-strands B3 and A5 in Xyn11, XylJ, XYNA, and XynB compared with Xyl1 (Fig. 1). Moreover, comparison of the structures of Xyl1 and Xyn11 highlighted many differences in the nature of the side-chains in the catalytic cavity and at the edge of the cleft. Actually, more charged residues are found in the alkalophilic Xyn11 and XylJ, whereas aromatic or neutral amino acids mostly occur in Xyl1. These charges were introduced in the catalytic site of Xyl1 by the Y16D, S18E, G50R, and Y186E substitutions. Some of these charges are also present in the weakly alkalophilic XYNA, but these substitutions were introduced singly or in combination in order to study the possible interdependence of their effects in a Xyl1 background. Furthermore, both charged residues, Lys54 and Glu57, located in the longer loop of Xyn11 and XylJ were introduced in Xyl1 by elongation of the existing loop. With the exception to Glu57, all these amino acids are naturally present in XYNA of *B. pumilus* A-30, whereas XynB of *D. thermophilum* Rt46B.1 already possesses the Glu18, Lys54, and Arg50 residues (Fig. 1). The single Y16D mutation yielded an unstable recombinant enzyme, while Y186E, as well as the mutants bearing the introduced loop portion, was inactive. Furthermore, none of the other mutations influenced the pH activity range of Xyl1, whereas in XylJ the simple reverse substitutions E18Q and E186Q drastically shifted the optimum pH from 9 to acidic values,

pH 6 for E18Q, and pH 5 for E186Q (Tamanoi et al. 1998). To a lesser extent, the D16N mutation decreased the activity of XylJ in the basic pH range. However, when the Y186E mutation was combined with S18E, G50R, or both in Xyl1, the activity of the resulting enzyme was restored (Table 2). In Xyn11, Glu18 is involved in the binding of the substrate and in a salt-bridge network with residues Arg50, Lys54, and Glu186 (Table 1). It seems that the charge modification of this residue in XylJ may redistribute the electronic cloud in the catalytic cleft. In regard to the broad shape of the activity profile of XYNA (Liu et al. 2002), this salt-bridge network may partly contribute to the alkaline activity adaptation. The role of Asp16 in XylJ remains obscure, but the substituted tyrosine in Xyl1 is known to play a role in substrate binding (Georis et al. 2000a). According to the small decrease in activity of mutant D16N at basic pH observed by Tamanoi et al. (1998), we have to consider the possible influence of this residue on the alkalophilic adaptation to occur by way of the binding of the substrate. Unfortunately, the instability resulting from the Y16D substitution in Xyl1 is presently not understood.

Superposition of the solved structures of Xyl1 and Xyn11 did not highlight any major differences in the conformation of the thumb of the two xylanases. However, two charged residues were exclusively found in or near the thumb of the two alkalophilic xylanases. Actually, Asp92 is located in the turn between β-strands B5 and B6, at the border of the palm, and Lys139 is located at the top of the thumb (Fig. 2D). Analysis of the structure of Xyn11 indicated that the former points to the solvent outside of the cleft, whereas the latter makes a salt-bridge with Glu57, which is situated in the longer loop of Xyn11. The sequence alignment showed that these two amino acids are surrounded by conserved motifs, in particular in the case of Asp92. These charged residues were introduced in Xyl1 by the N92D and E139K substitutions. Mutation N92D had no effect, whereas the inversion of charge obtained by the E139K substitution shifted the optimum pH activity of Xyl1 from pH 6 to pH 7.5. Most interestingly from a practical point of view, the E139K mutant exhibited specific activities of 1500 and 250 IU/mg of proteins at pH 9.0 and 10, respectively, conditions in which the wild-type enzyme is nearly inactive (<100 IU at pH 9.0 and close to zero at pH 10). However, when the E139K and N92D mutations were combined, the optimum pH value returned to that of the wild-type enzyme. Modeling experiments showed that the E139K mutation led to the elimination of the Glu139–Lys142 salt-bridge and highlighted the possible implication of the introduced Lys139 in an additional interaction with the substrate. Combination of this mutation with the N92D substitution probably leads to the establishment of a Lys139–Asp92 salt-bridge. The characterization of the two recombinant proteins bearing the loop elongation and the elongated loop combined with the E139K substitution could yield interesting information on the structural role of this longer β-strand in the alkalophilic adaptation. Unfortunately, none of these mutants were active. However, the E57Q substitution in XylJ yielded a recombinant protein with an activity profile similar to that of the wild-type, although the mutation eliminated the salt-bridge between this residue and Lys139 (Tamanoi et al. 1998). In order to compare the activity profiles of XylJ, Xyl1, and its mutants, we synthesized the sequence encoding the catalytic domain of XylJ (Fig. 3). This gene was designed with GC-rich codons so as to facilitate its expression in a *Streptomyces* host and was cloned behind the signal peptide coding sequence of the *xyl1* gene, in the construction used for production of the Xyl1 mutants. The synthesized XylJ presented an optimum activity near pH 7. This result deviated from the alkalophilic character previously described for XylJ. However, it seems that depending to the type of substrate used differences in activity profiles can occur. Actually, previous studies on the Xyn11 xylanase showed that the use of synthetic substrates like *o*-nitrophenyl β-xylobioside ($ONPX_2$) resulted in an optimum activity near pH 6, whereas pH 7–8 was observed with a more complex substrate such as xylan (Poon et al. 2003). Furthermore, deletion experiments highlighting the absence of influence of the C-terminal domain of XylJ on the catalytic activity led to a slight decrease of activity in the basic pH range (Kubo et al. 1996). Moreover, these data were obtained with larchwood xylan, whereas oats spelt xylan was used in the present work. Although the extent of this activity decrease remains to be established, these previous results could explain the pH activity profile observed here with the truncated XylJ. Nevertheless, in regard to all the observations made on XylJ and Xyn11 and the site-directed mutagenesis studies on XylJ, it should be carefully considered that the drastic shift in optimum pH induced by the sole E139K substitution in Xyl1 could be specific to this enzyme and the consequence of a different adaptation pathway from that responsible for the alkalophilic adaptation of XylJ. Actually, it has been previously described that an increase in the optimum pH could result from surprising substitutions of residues located in various parts of the enzyme. Indeed, recent work on the XynII xylanase of *T. reesei* has shown that the optimum pH is increased by 1 pH unit by the introduction of five arginine residues in the "Ser/Thr" surface of the enzyme (Turunen et al. 2002). Furthermore, directed evolution carried out on the xylanase of *Neocallimastix patriciarum* using the error-prone PCR method led to the widening of the pH activity range of the enzyme without causing a shift in the pH optimum (Chen et al. 2001). The various mutations were located throughout the structure but almost always outside the catalytic cleft. In addition, none of the substitutions described in these studies are present in the amino acid sequences of XylJ or Xyn11. Interestingly, directed evolution of the E186Q mutant of XylJ (described above) resulted in the recovery of the alkaline activity of the

mutant (Inami et al. 1994). In this case also, the observed substitutions were unexpected. All these observations clearly show that alkalophilic adaptation of xylanases can occur according to different pathways and that specific rules governing this type of evolution are difficult to establish.

Materials and methods

Bacterial hosts strains and plasmids

S. parvulus IMET41380 and the *Streptomyces* plasmid vector pIJ486 were gifts from Drs. D.A. Hopwood and T. Kieser (John Innes Institute, Norwich, UK). pDML 1011 and pDML1012 were used as previously described by Georis et al. (2000a). *Escherichia coli* DH5α was used as the host strain. The *E. coli–Streptomyces* shuttle plasmid was obtained by subcloning pDML1011 derivatives (obtained by site-directed mutagenesis) in the unique HindIII site of pIJ486. pCR-Script (Stratagene Ltd.) was used for cloning and sequencing of the synthetic *xylJ* gene.

Media, antibiotics, and culture conditions

Streptomyces liquid cultures were grown in YEME (Hopwood et al. 1985) and M13 media (Morosoli et al. 1986) on rotatory shakers at 220 rpm and 28°C. R2YE or minimal agar medium (Hopwood et al. 1985) was used for plating. The *E. coli* strains were grown at 37°C in Luria-Bertani broth. Thiostrepton (Squibb) was used at final concentrations of 25 μg/mL in liquid and solid media and 50 μg/mL in overlays. Ampicillin (Sigma Chemical) was used at 100 μg/mL.

After protoplast transformation by shuttle plasmids carrying the different mutations, Xyl1 recombinant proteins were produced as follow: 25 mL of 48-h cultures of *S. parvulus* in Tryptic Soy Broth (TSB) was used to inoculate 1 L of M13 medium with 1% xylose as the carbon source and 25 μg/mL of thiostrepton (Squibb). Cultures were grown in 1-L Erlenmeyer flasks containing 250 mL of medium and a stainless steel spring so as to improve oxygen transfer. These were incubated for 72 h at 28°C and 220 rpm on a rotary shaker. The production of xylanase was monitored at 8-h intervals.

Site-directed mutagenesis, cloning, and DNA sequencing of the xyl1 *gene*

Site-directed mutagenesis was performed on pDML1012 (Georis et al. 2000a) using the Quick-Change Site Directed Mutagenesis Kit from Stratagene according to the protocol recommended by the manufacturer and using the following primers (Pharmacia LKB):

Y16D (forward), GCACCAACAACGGCTACGACTACTCC TT CTGGACCGA;
Y16D (reverse), TCGGTCCAGAAGGAGTAGTCGTAGCCGTT GTTGGTGC;
S18E (forward), AACAACGGCTACTACTACGAGTTCTGGAC CGACGGCG;
S18E (reverse), CGCCGTCGGTCCAGAACTCGTAGTAGTAG CCGTTGTT;
V48L (forward), CGGCAACTTCCTCGCAGGCAAG;
V48L (reverse), CTTGCCTGCGAGGAAGTTGCCG;
G50R (forward), TTCGTCGCACGCAAGGGCTGGGCC;
G50R (reverse), GGCCCAGCCCTTGCGTGCGACGAA;
N83D (forward), GTGGACCGCCGACCCGCTGGTGGAGTAC;
N83D (reverse), GTACTCCACCAGCGGGTCGGCGGTCCAC;
A124Q (forward), CCGTCCGTCGAAGGCACCAAGAC;
A124Q (reverse), CTGGTTGACGCGGGTGGTCTGGTAGAC GTCGTACG;
E128K (forward), CCGTCCGTCAAGGGCACCAAGAC;
E128K (reverse), GGCGTTGACGCGGGTGGTCTGGTAG;
Y171E (forward), GGCAGCTTCAACTACGAGATGATCATG GCGACGGA;
Y171E (reverse), TCCGTCGCCATGATCATCTCGTAGTTGAA GCTGCC;
Y16D/S18E (forward), ACCAACAACGGCTACGACTACGAG TTCTGGACCGACGGC;
Y16D/S18E (reverse), GCCGTCGGTCCAGAACTCGTAGTCG TAGCCGTTGTTGGT;
"Loop" (forward), TGGGTCTGGGTCTCGTTGAACTTCTTGC CCTTGCCTGCGACGAAG; and
"Loop" (reverse), CCAGCAGGTCGGCAACATGAGCATCAAC TACTCCGGCAGTTTCAACCCC.

The PCR conditions used were: 5 min at 95°C, 15 times (30 sec at 95°C, 1 min at 55°C, 8 min at 72°C), and 3 min at 72°C. pDML 1012 derivatives were isolated using the GFX PCR DNA and Gel Band Purification Kit (Amersham Pharmacia Biotech Inc.), and double-stranded sequencing was carried with an Alf automated fluorescent DNA sequence (Pharmacia) using the dideoxynucleotide method and the Thermosequenase fluorescent DNA sequencing kit (Amersham) with universal and reverse primers.

Synthesis of the xylJ *gene by recursive PCR*

Synthesis of the *xylJ* gene was performed by recursive PCRs as described by Prodromou and Pearl (1992). Ten internal oligonucleotide primers representing the open reading frame of the *xylJ* gene sequence were designed so that overlapping regions yielded melting temperatures ranging from 51°C to 55°C. Only the coding sequence of the catalytic domain was synthesized since, as previously described (Nakamura et al. 1995), the C-terminal domain does not appear to influence the catalytic properties of the enzyme. The synthetic coding sequence naturally possessed eight unique restriction sites, whereas the two outermost primers (BSXJ-Start and BSXJ-End) containing the unique restriction sites BssHII at 5′ and BclI at 3′ were used to amplify and clone the gene. The primers used were:

BSXJ1 (85 bp): GCCATCACCTCCAACGAGATCGGCACCCA TGACGGCTACGACTACGAGTTCTGGAAGGACAGCGGC GGCAGCGGCTCCATGACCC;
BSXJ2 (85 bp): CTTGCCCTTGCGGAACAGGATGTTGTTGA CGTTGGACCACTGCGCCGAGAAGGTGCCGCCGGAGTT CAGGGTCATGGAGCCGCTG;
BSXJ3 (85 bp): CTGTTCCGCAAGGGCAAGAAGTTCGACGA GACCCAGACCCACCAGCAGATCGGCAACATGTCCATC AACTACGGCGCCACCTACA;
BSXJ4 (85 bp): TGTAGAACTCGACCAGCGGGTCCACGGTC CAGCCGTAGACGGTCAGGTAGGAGTTGCCGTTCGGGT TGTAGGTGGCGCCGTAGTT;
BSXJ5 (84 bp): CCGCTGGTCGAGTTCTACATCGTGGACTCC TGGGGCACCTGGCGGCCGCCGGGCGGGACCCCCAAG GGCACCATCAACGTCGAC;
BSXJ6 (85 bp): CGTCGCGGTCCCCTTGATGCTCGGCTGGTT GTAGCGGGTGGTCTCGTAGATCTGGTAGGTGCCCCCG TCGACGTTGATGGTGCCC;

BSXJ7 (85 bp): CAAGGGGACCGCGACGTTCCAGCAGTACT GGTCCGTCCGCACCTCCAAGCGCACCTCGGGCACCA TCTCCGTCAGCGAGCACTTC;
BSXJ8 (84 bp): CCTCGACGGTGAGCGCGACCTCGTACAT GTTGCCCATGTTCATGCCCAGGGACTCCCAGGCCCG GAAGTGCTCGCTGACGGAGA;
BSXJ9 (85 bp): GCGCTCACCGTCGAGGGCTACCAGTCGT CCGGCTCCGCCAACGTCTACTCCAACACGCTGACCAT CGGGGGCCAGTCGGGGGGGG;
BSXJ10 (64 bp): TCACGGGCCGCCCTTGGTCATGGACTCC GCCTCGACGCGCGTCGCCTGCTCCCCCCCCGACTGG;
BSXJ-Start (21 bp): GCGCGCGCGGCCATCACCTCC; and
BSXJ-End (22 bp): TGATCACGGGCCGCCCTTGGTC.

The conditions used for the recursive PCR were 5 min at 95°C, 30 times (2 min at 95°C; 2 min at 55°C; and 1 min at 72°C), and 10 min at 72°C. The reaction solution contained 38 pmole of the outermost oligonucleotides BSXJ-Start and BSXJ-End, 3.8 pmol of the internal oligonucleotides BSXJ1 to BSXJ10, 0.02 μmol dNTPs, 0.6 μmol $MgSO_4$, and 5 U Vent DNA polymerase in a total reaction volume of 100 μL. The PCR product was isolated from a low concentration gel using the GFX PCR DNA kit and purified with the Gel Band Purification Kit (Amersham Pharmacia Biotech, Inc.). The *xylJ* gene was then cloned into the pCR-Script vector (Stratagene Ltd.) and the nucleotide sequence was determined as described above.

Cloning of the synthetic xylJ

The synthesized 669 bp gene was cloned after the signal peptide DNA sequence of the *xyl1* gene and between the BssHII and BclI restriction sites so as to allow expression in the *S. parvulus* host (see Materials and Methods). Furthermore, in order to ensure correct processing of the fusion, the prediction of the cleavage site between the signal peptide and the mature protein was verified with the program SignalIP V.1.1 (http://www.cbs.dtu.dk/services/SignalP/).

Construction of the production vector for expression of the synthetic gene xylJ

The unique restriction site BssHII was introduced into pDML1011 at the 3′ end of the peptide signal of the *xyl1* gene, whereas the BclI restriction site was already present at 50 bp before the end of the gene. The introduction of BssHII was performed by PCR using the same conditions as were used for the site-directed mutagenesis (see above) and with the following oligonucleotides:

BssHII(A), cctggcacggcgcgcgc; and
BssHII(B), gcGCGCGCCGTGCCAGG.

The plasmid obtained was digested with BssHII and BclI, and the synthetic *xylJ* gene was inserted between these restriction sites. The production vector was an *E. coli–Streptomyces* shuttle plasmid resulting from the subcloning of the pDML1011 derivative in the unique HindIII site of pIJ486.

Xylanase assays

Endo-β-1,4-xylanase (EC 3.2.1.8) activity was measured by the dinitrosalicylic acid method (DNS) (Miller 1959); 40-μL aliquots of diluted enzyme were mixed with 360 μL of a 1% suspension of oat spelt xylan (Sigma Chemical Co.; Janssen) at different pHs and incubated for 10 min at 50°C. One international unit is defined as the amount of enzyme that releases 1 μmol of reducing sugar per minute. The pH dependence was determined using the following buffers: HCl/KCl 0.05 M (pH 2), sodium citrate 0.05 M (pH 2.5–6), sodium phosphate 0.05 M (pH 6–7), Tris/HCl 0.05 M (pH 7.5–9), and Na_2CO_3-$NaHCO_3$ 0.05 M (pH 9–11).

Proteins purification and analysis

Recombinant proteins of Xyl1

Culture supernatants (1 L) were harvested by centrifugation at 10,000*g* for 20 min and then microfiltered on 0.4-μm Millipore filters (Millipore) and diluted 10 times with water. After adjustment to pH 5.0, 300 g of moist CM-cellulose equilibrated in 10 mM sodium citrate buffer (pH 5.0) was added. The exchanger was washed with 3 L of the same buffer and harvested by decanting. Elution of recombinant enzymes was performed batch-wise with 1 L of 10 mM citrate buffer (pH 5.0) containing 1.5 M NaCl. Solutions were concentrated to 35 mL, dialyzed against 10 mM citrate buffer (pH 5.0), and loaded onto a Sulfopropyl Sepharose Fast Flow column (XK 26/40, 150 mL, Amersham Pharmacia Biotech). The enzyme was eluted with a linear NaCl gradient (450 mL) from 0–0.2 M, and fractions exhibiting xylanase activity were pooled and concentrated to 0.5 mg/mL.

Molecular masses were estimated by SDS–polyacrylamide gel electrophoresis (PAGE, Laemmli 1970).

XylJ

The culture supernatant (650 mL) was harvested as described above, and ammonium sulfate was added to 20% saturation. After standing overnight, the precipitate was recovered by centrifugation (30 min at 16.000*g*), dissolved in 75 mL of 10 mM Na_2HPO_4-NaH_2PO_4 buffer (pH 7), and dialyzed four times against 5 L of the same buffer for 6 h. The dialyzed solution was loaded onto a Q-Sepharose FF column (2.6 × 30 cm, 160 mL, Amersham Pharmacia Biotech) equilibrated with the same buffer. The column was eluted with a linear 0–500 mM NaCl (700 mL) gradient. Fractions of 10 mL were collected and assayed for xylanase activity. The active fractions were pooled, concentrated from 70 to 5 mL by ultrafiltration on a 10000 Da cut-off Amicon membrane, and applied to a Sephacryl S100 HR molecular sieve column (2.6 × 95 cm, 500 mL, Amersham Pharmacia Biotech) equilibrated in 20 mM Na_2HPO_4-NaH_2PO_4 buffer. The fractions exhibiting xylanolytic activity were collected and concentrated.

Amino acids numbering

The standard numbering used in the text results from the alignment numbering in Figure 1.

Modeling of the substrate

The structure of a xylo-oligosaccharide fragment containing eight sugars was modeled using the biopolymer module of the INSIGHTII program (MSI). The crystal structures of the *Bacillus circulans* xylanase complexed with xylotetraose (PDB code 1BCX; Wakarchuk et al. 1994) and 2-fluoro-xylose (PDB code 1BVV; Sidhu et al. 1999), and that of the *B. agaradhaerens* xylanase complexed with xylanopyranoside (PDB code 1QH7; Sa-

bini et al. 1999) were used as references for positioning the substrate in the active site of the *Streptomyces sp* S38 Xyl1 enzyme (PDB code 1HIX; Wouters et al. 2001). The structures of the four xylanases were superimposed by minimizing the root mean square deviations between the carbons of 12 residues bordering the active site. The two central units of the substrate were superimposed on the average position of the two xylose residues in the complexes. The six other xyloses (three in the direction of the nonreducing end and three in the direction of the reducing end) were manually oriented to cover hydrophobic areas in the binding cleft and to allow possible hydrogen bonding interactions. The geometries of the modeled enzyme-substrate complexes were optimized using the AMBER all atom force field (University of California, San Francisco), first by steepest descent energy minimization of atoms with forces >500 kcal/mol/Å and then by conjugate gradient energy minimization until the root-mean-square gradient was <0.1 kcal/mol/Å.

Modeling of the mutant E139K

In the Xyl1 E139K mutant, replacement of Glu139 by a lysine was performed with the Biopolymer module of the InsightII software. Subsequent conformational analysis around the rotatable bonds of the lysine side-chain did not allow unambiguous determination of the orientation of the residue. The energy of the corresponding complexes was minimized with the use of CNDO charges to compute the Coulombic term. Dielectric function used in calculating the electrostatic energy was distance dependent. This is used to mimic the presence of a highly dielectric solvent.

Acknowledgments

This work was supported in part by Ministry of Walloon Region, Department of Technology Research and Energy (conventions Bioval 1 no. 981/3860 and np. 981/3709), by the FNRS (Brussels, Belgium, FRFC contract nos.; 2.4508.01 and 2.4524.03 and LOT. NAT.9.4538.03.) F.d.L.E. is a fellow of the Fonds pour la Formation à la Recherche dans l'Industrie et l'Agriculture (FRIA, Brussels, Belgium). We thank Drs. J. Georis, T. Collins, M. Galleni, A. Matagne, and F. Bouillenne for their helpful advice.

References

Chen, Y.L., Tang, T.Y., and Cheng, K.J. 2001. Directed evolution to produce an alkalophilic variant from a *Neocallimastix patriciarum* xylanase. *Can. J. Microbiol.* **47:** 1088–1094.

Collins, T., Gerday, C., and Feller, G. 2004. Xylanases, xylanase families and extremophilic xylanases. *FEMS Microb. Rev.* (in press).

de Lemos Esteves, F., Ruelle, V., Lamotte-Brasseur, J., Quinting, B., and Frere, J.M. 2004. Acidophilic adaptation of family 11 endo-β-1,4-xylanases: Modeling and mutational analysis. *Protein Sci.* **13:** 1209–1218.

Dominguez, R., Souchon, H., Spinelli, S., Dauter, Z., Wilson, K.S., Chauvaux, S., Beguin, P., and Alzari, P.M. 1995. A common protein fold and similar active site in two distinct families of β-glycanases. *Nat. Struct. Biol.* **2:** 569–576.

Fushinobu, S., Ito, K., Konno, M., Wakagi, T., and Matsuzawa, H. 1998. Crystallographic and mutational analyses of an extremely acidophilic and acid-stable xylanase: Biased distribution of acidic residues and importance of Asp37 for catalysis at low pH. *Protein Eng.* **11:** 1121–1128.

Georis, J., de Lemos Esteves, F., Lamotte-Brasseur, J., Bougnet, V., Devreese, B., Giannotta, F., Granier, B., and Frere, J.M. 2000a. An additional aromatic interaction improves the thermostability and thermophilicity of a mesophilic family 11 xylanase: Structural basis and molecular study. *Protein Sci.* **9:** 466–475.

Georis, J., Giannotta, F., De Buyl, E., Granier, B., and Frère, J. 2000b. Purification and properties of three endo-β-1,4-xylanases produced by *Streptomyces* sp. strain S38 which differ in their ability to enhance the bleaching of kraft pulps. *Enzyme Microb. Technol.* **26:** 178–186.

Harris, G.W., Pickersgill, R.W., Connerton, I., Debeire, P., Touzel, J.P., Breton, C., and Perez, S. 1997. Structural basis of the properties of an industrially relevant thermophilic xylanase. *Proteins* **29:** 77–86.

Henrissat, B. and Davies, G. 1997. Structural and sequence-based classification of glycoside hydrolases. *Curr. Opin. Struct. Biol.* **7:** 637–644.

Hopwood, D.A., Bidd, M.J., Chater, K.F., Kieser, T., Bruton, C.J., Kieser, H.M., Lydiate, D.J., Smith, C.P., Ward, J.M., and Shrempf, H. 1985. *Genetic manipulation of* Streptomyces: *A laboratory manual.* The John Innes Foundation, Norwich.

Inami, M., Morokuma, C., Sugio, A., Tamanoi, H., Yatsunami, R., and Nakamura, S. 2003. Directed evolution of xylanase J from alkaliphilic *Bacillus* sp. strain 41M-1: Restore of alkaliphily of a mutant with an acidic pH optimum. *Nucleic Acids Res. Suppl.* 315–316.

Irwin, D., Jung, E.D., and Wilson, D.B. 1994. Characterization and sequence of a *Thermomonospora fusca* xylanase. *Appl. Environ. Microbiol.* **60:** 763–770.

Joshi, M.D., Sidhu, G., Pot, I., Brayer, G.D., Withers, S.G., and McIntosh, L.P. 2000. Hydrogen bonding and catalysis: A novel explanation for how a single amino acid substitution can change the pH optimum of a glycosidase. *J. Mol. Biol.* **299:** 255–279.

Kluepfel, D., Vats-Mehta, S., Aumont, F., Shareck, F., and Morosoli, R. 1990. Purification and characterization of a new xylanase (xylanase B) produced by *Streptomyces lividans* 66. *Biochem. J.* **267:** 45–50.

Kubo, T., Nakai, R., Tamanoi, H., Wakabayashi, K., and Nakamura, S. 1996. Characterization of the additional C-terminal domain of xylanase J from alkaliphilic *Bacillus* sp. strain 41M-1. *Nucleic Acids Symp. Ser.* **35:** 221–222.

Kulkarni, N., Shendye, A., and Rao, M. 1999. Molecular and biotechnological aspects of xylanases. *FEMS Microbiol. Rev.* **23:** 411–456.

Laemmli, U.K. 1970. Cleavage of structural proteins during the assembly of the head of bacteriophage T4. *Nature* **227:** 680–685.

Liu, X., Qu, Y., You, F., and Liu, Y. 2002. Studies on the key amino acid residues responsible for the akali-tolerance of the xylanase by site-directed or random mutagenesis. *J. Mol. Cat. B* **18:** 307–313.

Mazy-Servais, C., Moreau, A., Gerard, C., and Dusart, J. 1996. Cloning and nucleotide sequence of a xylanase-encoding gene from *Streptomyces* sp. strain EC3. *DNA Seq.* **6:** 147–158.

Miao, S., Ziser, L., Aebersold, R., and Withers, S.G. 1994. Identification of glutamic acid 78 as the active site nucleophile in *Bacillus subtilis* xylanase using electrospray tandem mass spectrometry. *Biochemistry* **33:** 7027–7032.

Miller, G.L. 1959. Use of dinitrosalicylic acid reagent for determination of reducing sugar. *Anal. Chem.* **31:** 426–428.

Morosoli, R., Bertrand, J.L., Mondou, F., Shareck, F., and Kluepfel, D. 1986. Purification and properties of a xylanase from *Streptomyces lividans*. *Biochem. J.* **239:** 587–592.

Morris, D.D., Gibbs, M.D., Chin, C.W., Koh, M.H., Wong, K.K., Allison, R.W., Nelson, P.J., and Bergquist, P.L. 1998. Cloning of the xynB gene from *Dictyoglomus thermophilum* Rt46B.1 and action of the gene product on kraft pulp. *Appl. Environ. Microbiol.* **64:** 1759–1765.

Nakamura, S., Wakabayashi, K., Nakai, R., Aono, R., and Horikoshi, K. 1993. Purification and some properties of an alkaline xylanase from alkaliphilic *Bacillus* sp. strain 41M-1. *Appl. Environ. Microbiol.* **59:** 2311–2316.

Nakamura, S., Nakai, R., Namba, K., Kubo, T., Wakabayashi, K., Aono, R., and Horikoshi, K. 1995. Structure-function relationship of the xylanase from alkaliphilic *Bacillus* sp. strain 41M-1. *Nucleic Acids Symp. Ser.* 99–100.

Poon, D.K., Webster, P., Withers, S.G., and McIntosh, L.P. 2003. Characterizing the pH-dependent stability and catalytic mechanism of the family 11 xylanase from the alkalophilic *Bacillus agaradhaerens*. *Carbohydr. Res.* **338:** 415–421.

Prodromou, C. and Pearl, L.H. 1992. Recursive PCR: A novel technique for total gene synthesis. *Protein Eng.* **5:** 827–829.

Sabini, E., Sulzenbacher, G., Dauter, M., Dauter, Z., Jorgensen, P.L., Schulein, M., Dupont, C., Davies, G.J., and Wilson, K.S. 1999. Catalysis and specificity in enzymatic glycoside hydrolysis: A 2,5B conformation for the glycosyl-enzyme intermediate revealed by the structure of the *Bacillus agaradhaerens* family 11 xylanase. *Chem. Biol.* **6:** 483–492.

Sidhu, G., Withers, S.G., Nguyen, N.T., McIntosh, L.P., Ziser, L., and Brayer, G.D. 1999. Sugar ring distortion in the glycosyl-enzyme intermediate of a family G/11 xylanase. *Biochemistry* **38:** 5346–5354.

Singh, S., Madlala, A.M., and Prior, B.A. 2003. *Thermomyces lanuginosus*: Properties of strains and their hemicellulases. *FEMS Microbiol. Rev.* **27:** 3–16.

Subramaniyan, S. and Prema, P. 2000. Cellulase-free xylanases from *Bacillus* and other microorganisms. *FEMS Microbiol. Lett.* **183:** 1–7.

Tamanoi, H., Kasahara, S., Kuroda, T., Kubo, T., Nakai, R., Namba, K., Wakabayashi, K., and Nakamura, S. 1998. Role of acidic amino acids in the akaline pH optimum of xylanase J from alkaliphilic *Bacillus* sp. strain 41M-1. *Nucleic Acids Symp. Ser.* **39:** 205–206.

Torronen, A., Mach, R.L., Messner, R., Gonzalez, R., Kalkkinen, N., Harkki, A., and Kubicek, C.P. 1992. The two major xylanases from *Trichoderma reesei*: Characterization of both enzymes and genes. *Biotechnology* **10:** 1461–1465.

Torronen, A., Harkki, A., and Rouvinen, J. 1994. Three-dimensional structure of endo-1,4-β-xylanase II from *Trichoderma reesei*: Two conformational states in the active site. *EMBO J.* **13:** 2493–2501.

Turunen, O., Vuorio, M., Fenel, F., and Leisola, M. 2002. Engineering of multiple arginines into the Ser/Thr surface of *Trichoderma reesei* endo-1,4-β-xylanase II increases the thermotolerance and shifts the pH optimum towards alkaline pH. *Protein Eng.* **15:** 141–145.

Viikari, L., Kantelinen, A., Sundquist, J., and Linko, M. 1994. Xylanases in bleaching: From an idea to the industry. *FEMS Microbiol. Rev.* **13:** 335–350.

Wakarchuk, W.W., Campbell, R.L., Sung, W.L., Davoodi, J., and Yaguchi, M. 1994. Mutational and crystallographic analyses of the active site residues of the *Bacillus circulans* xylanase. *Protein Sci.* **3:** 467–475.

Wong, K.K., Tan, L.U., and Saddler, J.N. 1988. Multiplicity of β-1,4-xylanase in microorganisms: Functions and applications. *Microbiol. Rev.* **52:** 305–317.

Wouters, J., Georis, J., Engher, D., Vandenhaute, J., Dusart, J., Frere, J.M., Depiereux, E., and Charlier, P. 2001. Crystallographic analysis of family 11 endo-β-1,4-xylanase Xyl1 from *Streptomyces* sp. S38. *Acta Crystallogr. D Biol. Crystallogr.* **57:** 1813–1819.

Yang, R.C., MacKenzie, C.R., Bilous, D., and Narang, S.A. 1989. Hyperexpression of a *Bacillus circulans* xylanase gene in *Escherichia coli* and characterization of the gene product. *Appl. Environ. Microbiol.* **55:** 1192–1195.